Improving the size uniformity of dendritic fibrous nano-silica by a facile one-pot rotating hydrothermal approach

Yabin Wang,†* Keke Hu,† Juan He and Yantu Zhang

Shaanxi Key Laboratory of Chemical Reaction Engineering, College of Chemistry and Chemical Engineering, Shengdi Road 580, Yan'an University, Yan'an 716000, Shaanxi, P. R. China.

E-mail addresses: ybw_bingerbingo@126.com (Y. B. Wang)

†These authors contributed equally to this work.

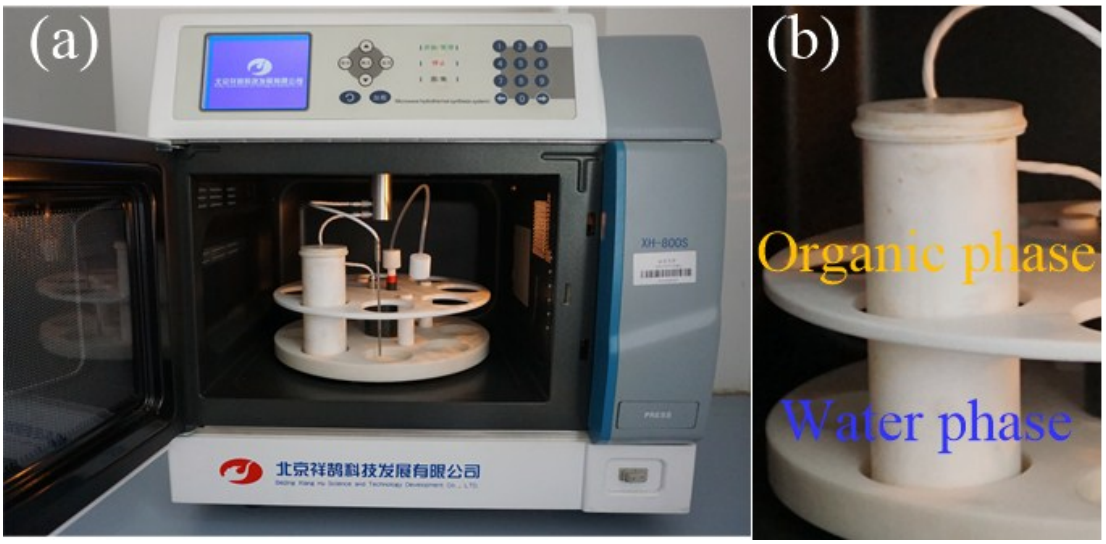

Fig. S1 A microwave-assisted hydrothermal system for KCC-1 fabrication. Organic phase mainly is cyclohexane (See synthesis process of experimental details).

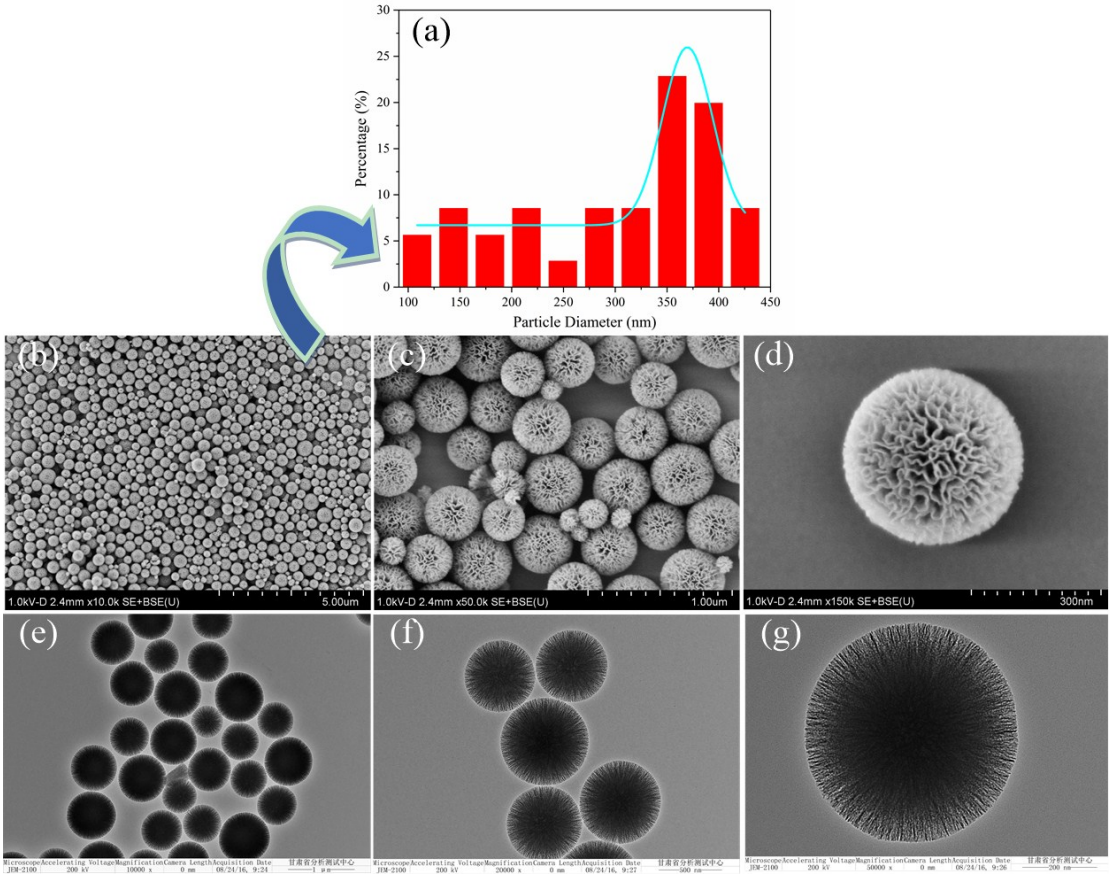

Fig. S2 Diameter distribution curve of KCC-1 extracted from SEM image with a large scale of 5 μm (b) where over 350 nanospheres are counted and analyzed. SEM (b-d) and TEM (e-g) images of KCC-1 prepared by following the same synthesis process of the milestone investigation from Polshettiwar *et al* [1].

Fig. S3 A one-pot rotating hydrothermal system for KCC-1 fabrication. Organic phase mainly is cyclohexane (See synthesis process of experimental details).

Table S1 The range value of diameter distribution (the interval difference *Δ*), the symmetry of distribution percentage referred to the fitted line, KCC-1 uniformity, the top three percentages in diameter distribution range, and peculiar morphology evaluation (broken or immature) of KCC-1 synthesized by a facile one-pot rotating hydrothermal approach with different stirring rates.

Stirring rate (rpm)	**0**	**30**	**60**	**90**	**120**	**150**
Range value (nm) (interval Δ)	200-725 (525)	275-650 (375)	275-575 (300)	300-575 (275)	375-775 (400)	350-650 (300)
Symmetry	medium	medium	excellent	medium	good	good
Uniformity	poor	medium	excellent	good	good	good
Top three percentages	575-600 (16.0%); 550-575 (15.7%); 525-550 (15.4%)	450-475 (20.4%); 500-525 (16.4%); 550-575 (16.4%)	450-475 (27.8%); 425-450 (16.3%); 475-500 (14.2%)	400-425 (23.4%); 425-450 (15.7%); 500-525 (14.6%)	500-525 (29.5%); 450-475 (23.0%); 475-500 (18.9%)	500-525 (21.3%); 450-475 (18.5%); 475-500 (17.5%)
Broken particles	some	none	none	none	none	some
Immature particles	some	few	few	few	some	some

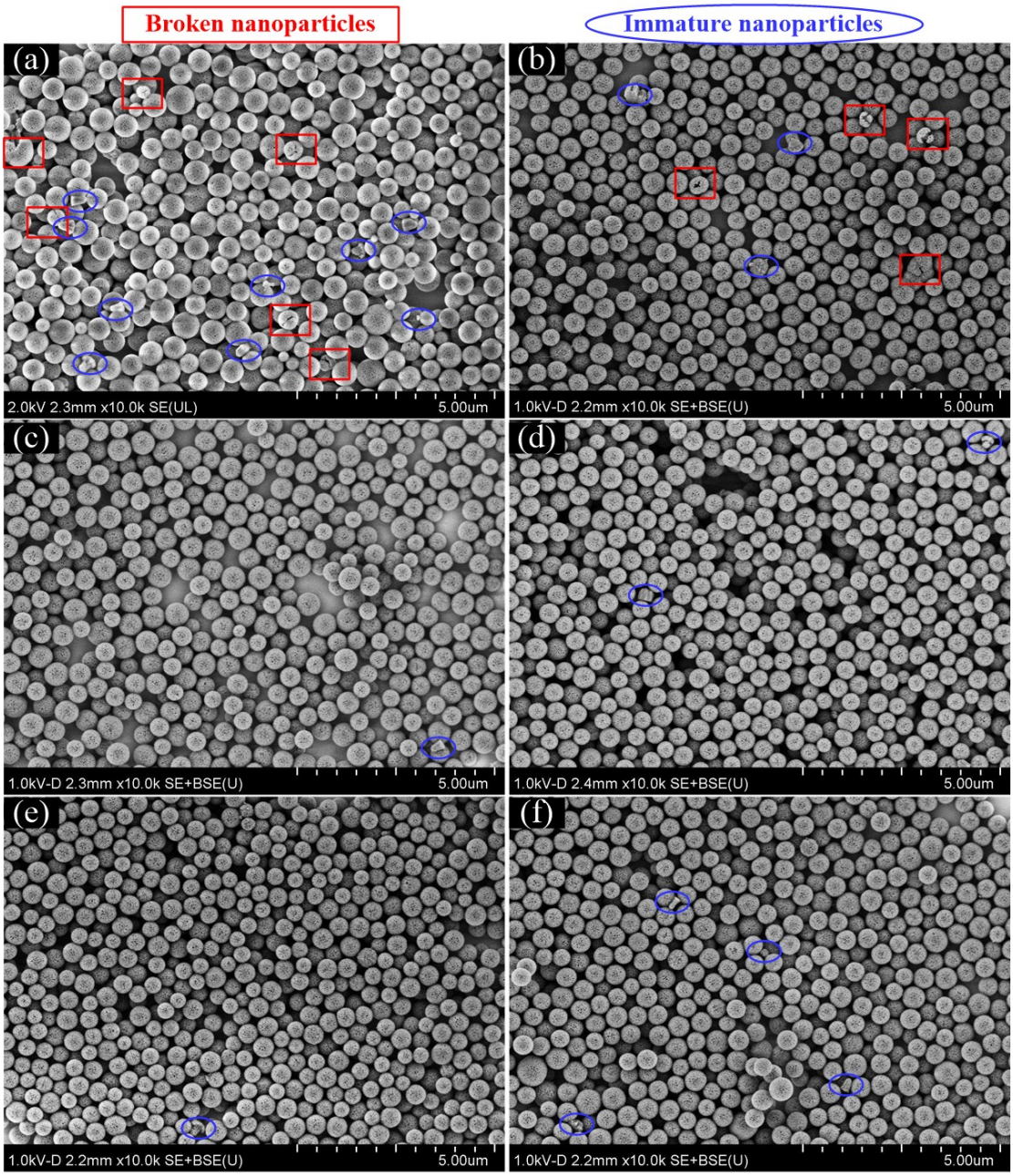

Fig. S4 SEM images of KCC-1 synthesized by a facile one-pot rotating hydrothermal approach with different stirring rates of 0 (a), 150 (b), 30 (c), 60 (d), 90 (e), and 120 rpm (f), respectively.

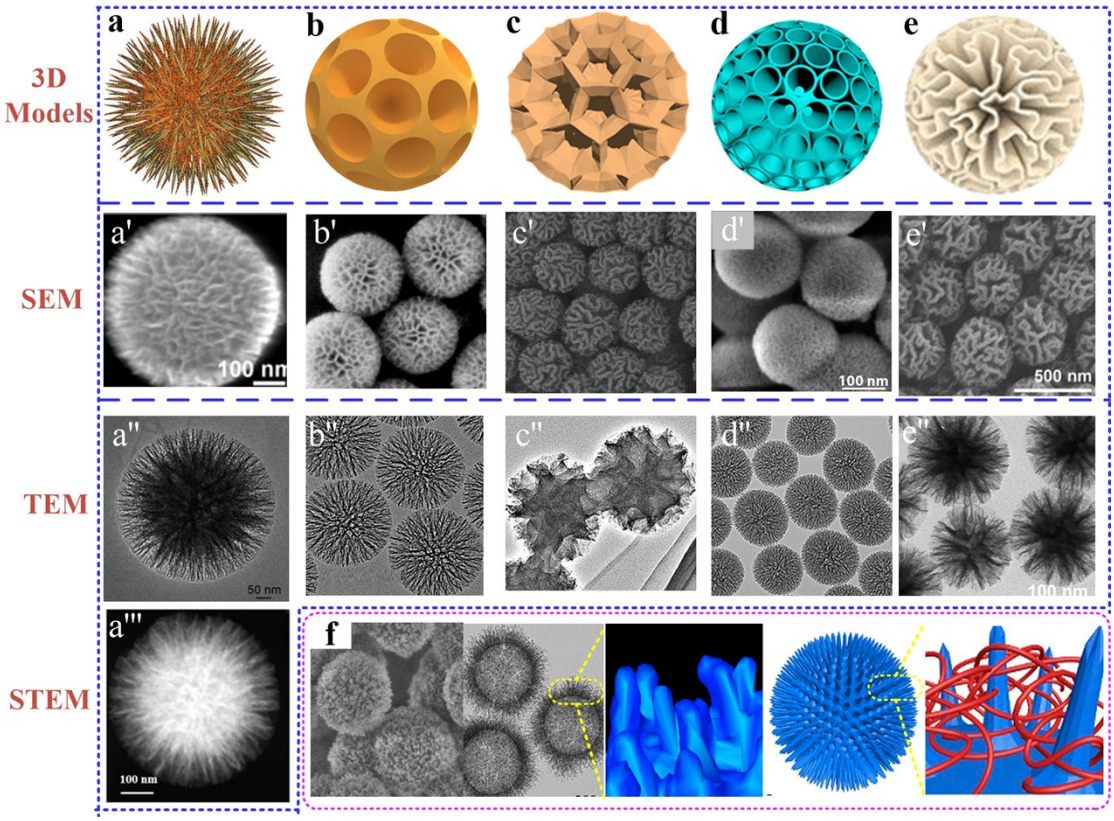

Fig. S5 Some typically simulated 3D structural models of KCC-1 nanosphere from teams of Vivek Polshettiwa (a) [2] Dongyuan Zhao (b) [3], Xin Du (c) [4], Chengzhong Yu (d) [5], and Jin Soo Kang (e) [6], respectively. Actual seaurchin-like silica nanoparticles of rambutan-like morphologies with spike-type subunit from team of Chengzhong Yu (f) [5]. Reproduced from ref. 2 with permission from American Chemical Society, copyright 2016. Reproduced from ref. 3 with permission from American Chemical Society, copyright 2014. Reproduced from ref. 4 with permission from John Wiley and Sons, copyright 2017. Reproduced from ref. 5 with permission from American Chemical Society, copyright 2017. Reproduced from ref. 6 with permission from Springer Nature Limited, copyright 2016.

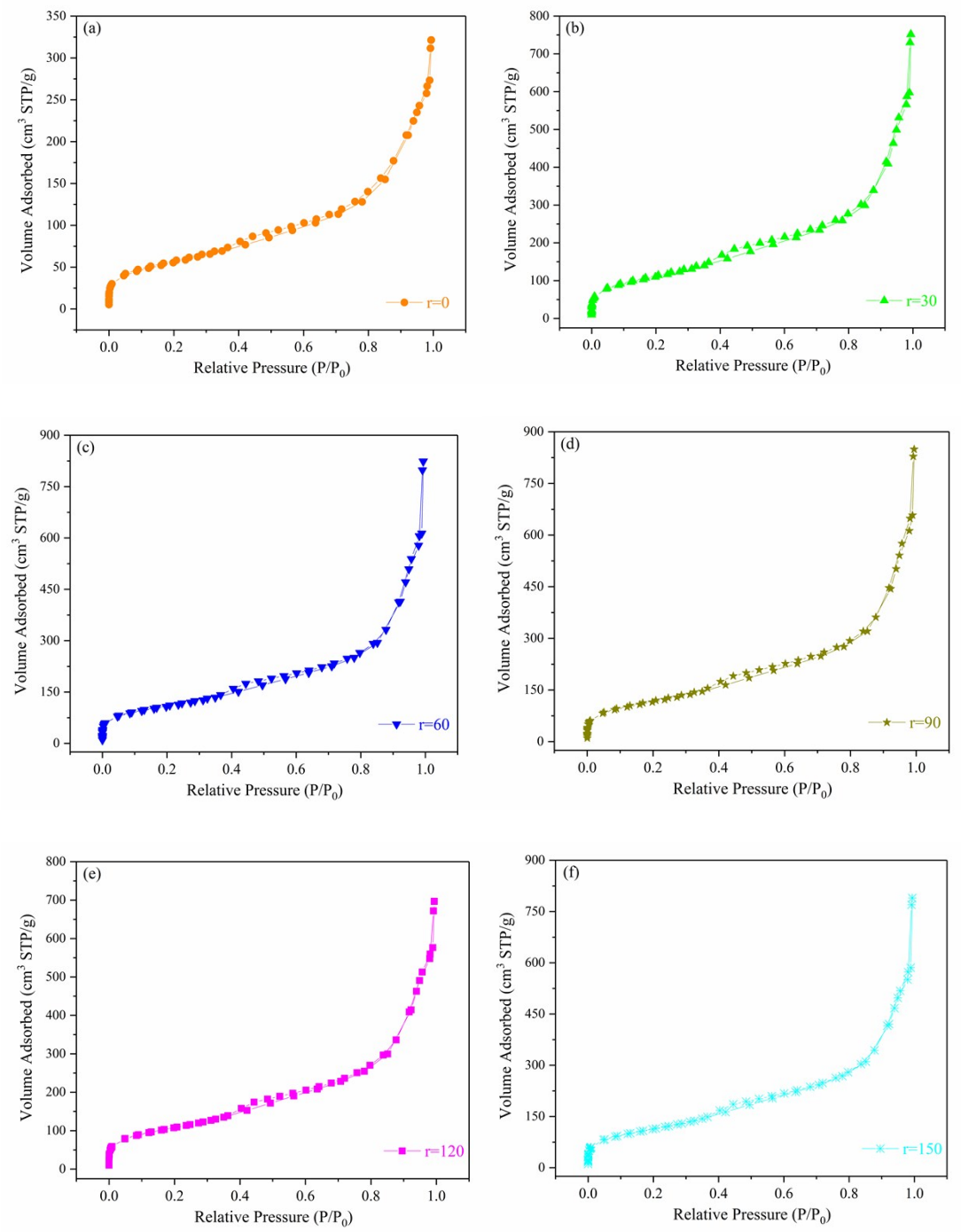

Fig. S6 N_2 adsorption-desorption isotherms of KCC-1 synthesized by a facile one-pot rotating hydrothermal approach with different stirring rates 0 (a), 30 (b), 60 (c), 90 (d), 120 (e), and 150 rpm (f), respectively.

Table S2 The BET surface area (S_{BET}), pore volume (V_P), and the main pore distribution of KCC-1 synthesized by a facile one-pot rotating hydrothermal approach with different stirring rates.

Stirring rate (rpm)	**0**	**30**	**60**	**90**	**120**	**150**
S_{BET} (m^2/g)	202.562	402.676	421.374	387.642	389.467	413.774
V_P (cm^3/g)	0.4973	1.163	1.314	1.274	1.078	1.221
Main pore distribution (nm)	2-5; 11-15	2-5; 11-15	2-5; 11-15	2-5; 11-15	2-5; 11-15	2-5; 11-15

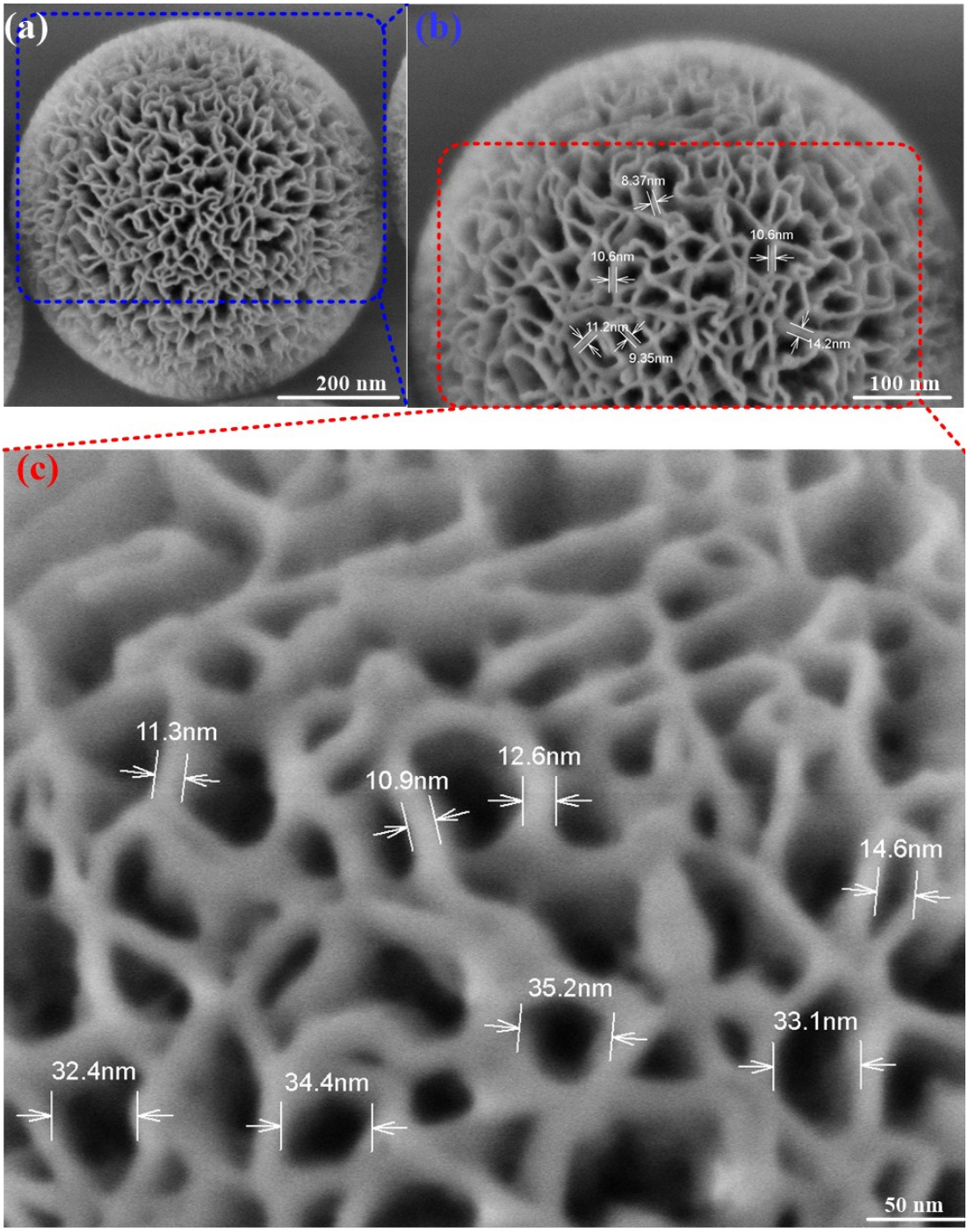

Fig. S7 SEM images of a KCC-1 nanosphere with different magnifications of 200 nm (a), 100 nm (b), and 50 nm (c).

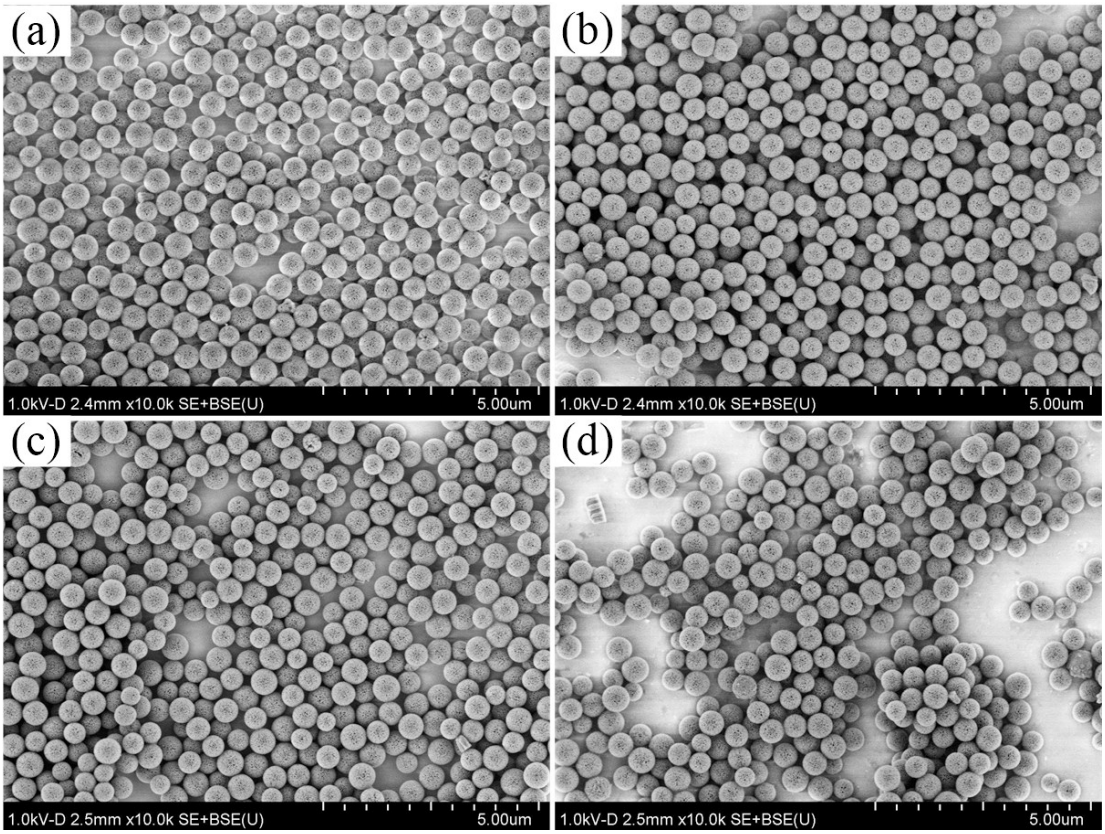

Fig. S8 SEM images of KCC-1 nanospheres from random four parallel tests.

Notes and references

[1] V. Polshettiwar, D. Cha, X. Zhang, M.B. Jean, High-surface-area silica nanospheres (KCC-1) with a fibrous morphology, Angew. Chem. Int. Edit., 49 (2010) 9652-9656.

[2] R. Singh, R. Bapat, L. Qin, H. Feng, V. Polshettiwar, Atomic layer deposited (ALD) TiO_2 on fibrous nano-silica (KCC-1) for photocatalysis: nanoparticle formation and size quantization effect, ACS Catal., 6 (2016) 2770-2784.

[3] D. Shen, J. Yang, X. Li, L. Zhou, R. Zhang, W. Li, L. Chen, R. Wang, F. Zhang, D. Zhao, Biphase stratification approach to three-dimensional dendritic biodegradable mesoporous silica nanospheres, Nano Lett., 14 (2014) 923-932.

[4] X. Du, C. Zhao, X. Li, H. Huang, J. He, Y. Wen, X. Zhang, Smart design of small Pd nanoparticles confined in hollow carbon nanospheres with large center-radial mesopores, Eur. J. Inorg. Chem., 2017 (2017) 2517-2524.

[5] H. Song, M. Yu, Y. Lu, Z. Gu, Y. Yang, M. Zhang, J. Fu, C. Yu, Plasmid DNA delivery: nanotopography matters, J. Am. Chem. Soc., 139 (2017) 18247-18254.

[6] J.S. Kang, J. Lim, W.Y. Rho, K. Jin, D.S. Moon, J. Jeong, D. Jung, J.W. Choi, J.K. Lee, Y.E. Sung, Wrinkled silica/titania nanoparticles with tunable interwrinkle distances for efficient utilization of photons in dye-sensitized solar cells, Sci. Rep., 6 (2016) 30829.